

# Electromigration-induced surface evolution in bamboo lines with transgranular and intergranular edge voids

Menachem Nathan<sup>a\*</sup>, Amir Averbuch<sup>b</sup>, Moshe Israeli<sup>c</sup>

<sup>a</sup>Department of Electrical Engineering - Physical Electronics

Tel Aviv University, Tel Aviv 69978, Israel

<sup>b</sup>School of Computer Science, Tel Aviv University, Tel Aviv 69978, Israel

<sup>c</sup>Faculty of Computer Science, Technion, Haifa 32000, Israel

\*Corresponding author: nathan@eng.tau.ac.il

## Abstract

The evolution of a surface intersected by transgranular and intergranular edge voids under isotropic surface diffusion and electric field effects is simulated numerically under both mass-conserving and non-mass-conserving boundary conditions. A surprising similarity is found in the surface topology of transgranular voids between our non-mass-conserving model and Schimschak and Krug's (J. Appl. Phys. 87 (2000) 695) mass-conserving model. The electric field is found to slow the development of an intergranular groove along a positively tilted grain boundary, and to cause thinning or thickening of grains under non-mass-conserving conditions.

**Keywords:** Electromigration, surface evolution, simulation, modeling.

## 1 Introduction

The evolution of a surface subjected to surface diffusion and electromigration (EM) is of obvious interest in microelectronic technologies. Although the so-called grooving/surface diffusion Mullins problem [1] has been around for quite a while, its numerical treatment and simulation is much more recent [2]. The EM-driven evolution of a transgranular

(TG) edge void has been treated numerically by a number of researchers [3]-[5], while that of intergranular (IG) edge voids in “bamboo” metal lines has received scant attention [6]. In the closest study to ours, Schimschak and Krug [3, 4] proposed a continuum description of an EM-induced surface evolution of a TG edge void in a top conductive surface of a line in which the bottom surface is insulating. The computational domain was a finite strip with a length/thickness ratio of 3.9, and with periodic boundary conditions in the current direction. The aim of this letter is to present selected results of the evolution of a surface having either a TG or an IG edge void, under the action of isotropic surface diffusion alone or in combination with an electric field, when the numerical approach uses two different types of boundary conditions. The TG void surface evolution is then compared with that in Fig. 4 of [4]. The IG void results have no similar literature comparison base. The theoretical formulation of the mass-conserving version of our model and the numerical techniques employed are presented in detail in a separate paper [7].

## 2 Model

Consider the single grain and two-grain domains shown respectively in Figs. 1)a and 1b, representing a thin metal strip attached to an insulating substrate and attached to electrodes at its ends A and B. The representation is two-dimensional in the  $x - y$  plane, the line being uniform (one grain wide) in the  $z$ -direction. Vector  $\vec{E}$  indicates an external electric field, positive in the  $+x$  direction, and opposite to an electron “wind”. Edge voids are assumed only on the top conducting curvilinear surface A-B. In Fig. 1b, a planar grain boundary (GB) TC is pinned at the substrate.  $T$  is a top triple point. Equal angles  $\theta_1 = \theta_2$  reflect an assumed isotropic surface energy.  $L_x$  (domain or line length) /  $L_y$  (line thickness) = 6 in all simulations. The top interface moves in its normal direction  $\vec{n}$  with a known speed function  $F$ . The front velocity includes surface diffusion and EM components, which depend respectively on the second derivatives of the interface curvature  $K$  and of the voltage  $U$ , taken with respect to the present interface arclength  $s$ :

$$F = BK_{ss} + \alpha U_{ss} \quad (2.1)$$

Constant positive coefficients  $B$  and  $\alpha$  express respectively the contribution of the (isotropic) diffusion and the field forces. Normalizing the physical time of the problem

$\tau = Bt$ , one can assume  $B = 1$  without any loss of generality. The curved grain-void boundary is set parametrically in the Cartesian space:

$$x = x(r) \quad y = y(r) \quad (2.2)$$

where  $r$  is a parameter independent of time. The evolution equations are:

$$\dot{x} = F \frac{\dot{y}}{g} \quad \dot{y} = -F \frac{\dot{x}}{g} \quad (2.3)$$

where dot ( $\dot{\phantom{x}}$ ) denotes time derivative, and prime denotes spatial derivative (with respect to  $r$ ). The present arclength cannot be used as a parameter since it is time-dependent, but we can use the  $s$  of the initial or of another reference configuration.  $g$  is a metric function, defined as

$$g = \frac{ds}{dr} = \sqrt{x^2 + y^2}. \quad (2.4)$$

The boundary conditions are set at end points  $A$  and  $B$ . For a two-grain domain, the triple point behavior is defined in [7]. Two different physical cases are considered:

**Non-mass-conserving case A:**  $A$  and  $B$  are assumed far from any irregularities, virtually at infinity. Therefore, the slopes are assumed zero at these points, and the first derivative of curvature  $K$  with respect to  $s$  vanishes:

$$\frac{dx}{ds} = -1 \quad \frac{dy}{ds} = 0 \quad K_s = 0. \quad (2.5)$$

The contour is passed counter-clockwise, and  $s$  increases when moving from  $A$  to  $B$ . At infinity, the arclength is time-independent.  $K_s = 0$  in Eq. 2.5 implies perfect insulation with respect to flow or exchange of matter between surroundings and domain when the electric field gradient is absent at the external boundaries.

**Mass-conserving case B:** The flux at  $A$  and  $B$  is considered to be zero:

$$K_s^A + \alpha U_s^A = 0, \quad K_s^B + \alpha U_s^B = 0. \quad (2.6)$$

Thus,  $K_s$  at these points does not vanish, but rather proportional to the electric field. As in case A,  $\frac{dx}{ds} = -1$  and  $\frac{dy}{ds} = 0$ .

In Figs. 2-5, case A is shown in (a), and case B in (b).

### 3 Results and discussion

Figure 2 shows the evolution of a top surface with a left and a right TG void, both initially triangular. Figure 2a shows results for case A with a strong field ( $\alpha = 50$ ), and Fig. 2b results for case B with a moderate field ( $\alpha = 20$ ). The field strength was found to have a relatively weak qualitative influence [7], allowing comparison between the two. Each starting void has one perpendicular facet and one positively ( $\vec{E} \cdot \vec{n} < 0$ ) or negatively ( $\vec{E} \cdot \vec{n} > 0$ ) tilted facet vs. the electric field, similar to the void faceting in [5]. With time, in case A, the left void develops a topology of horizontal slit and overhang essentially identical with that of Fig. 4 in [4], in spite of the different boundary conditions. The right void shows a similar slit but little overhang, which however may still develop with additional time. As in [5], the slits of both voids extend in the +E direction, with the negatively tilted void advancing faster. In case B, no overhang is seen in any void, both voids moving to the right as in case A and in [5] and seemingly becoming shallower with time. Matter is removed from the right edge (cathode), and accumulates at the left edge (anode). The weak dependence of the surface evolution on the initial void facet orientation is in agreement with [5], despite the different problem formulations here and in [5]. Therein, the problem followed is the surface evolution of a side-wall void, with both side walls being conducting.

Figure 3 shows the evolution of a top surface intersected by a positively tilted ( $\beta = \pi/4$ ) GB under surface diffusion alone ( $\alpha = 0$ ). Case A (a) is followed to 20M time-steps, while case B (b) is followed to 200K only. In both cases, material removed from the right grain near the triple point accumulates on the left grain. The triple point moves down and to the left, the two GBs defining there a GB groove. The local thinning leads eventually to line failure. The profile at time step 200K in (b) is similar to that of time-step 300K in (a). It is likely that further in time, (b) will show a deepening GB groove similar to (a), but no left grain thickening.

Figure 4 shows the evolution of a surface as in Fig. 3, but with the addition of a weak electric field ( $\alpha = 10$ ). Case A (a) is followed to 20M time-steps, while B (b) is followed only to 140K. The topology in (a) shows a thinned right grain, and an unthinned left grain. As in Fig. 3a, the triple point moves down and to the left. In (b), both grain thicknesses and the triple point position remain practically unchanged to time-step 140K, but, as in Fig. 2b, material is removed at the right line boundary and added at the left one. Increasing the electric field or the GB tilt does not materially

change the picture [7]. Relative to Fig. 3b after equal time (not shown), the GB groove in Fig. 4b is somewhat shallower, indicating that in a surface with a positively tilted boundary the electric field has a “healing” effect, acting against surface diffusion.

The simulation stops automatically at time step 140K when the line is “cut” or breaks at the right boundary due to material removal. In contrast with a real drift velocity experiment, in which the right domain boundary (cathode edge) moves while current is introduced to the line from a high resistivity underlayer, the present simulation uses a fixed domain boundary. We do not think that longer simulations will materially change the profiles seen in the mass-conserving model.

Figure 5 shows the evolution of a top surface intersected by a negatively tilted ( $\beta = 3\pi/4$ ) grain boundary in a weak electric field ( $\alpha = 10$ ). In contrast with Fig. 4a, the topology in Fig. 5a shows accumulation of material in the right grain, while the left grain remains unchanged. The triple point is now stationary even after 20M time-steps. The topology in Fig. 5b shows now, in addition to cathode mass removal and anode accumulation, a deepening of the GB groove relative to Fig. 4b, with the triple point moving down and to the right faster than in a positively tilted GB. As in Fig. 4b, the simulation stops automatically at time step 137K because the cathode edge is eaten away.

For a brief discussion of our simulation results, we first note that EM experiments on metal lines are performed in both mass-conserving and non-mass-conserving setups. Thus, a resistance change or lifetime experiment in a line connected between practically infinite reservoirs does not necessarily conserve the line material, while a drift velocity experiment is mass-conserving. Selective surface thinning is seen in resistance change/lifetime experiments [8, 9], qualitatively in agreement with our case A model for positively tilted GBs. However, there is no experimental evidence for the grain thickening predicted in Fig. 5a. Uneven and selective thinning along a line subjected to EM may thus result from different GB tilts. Our mass-conserving model simulations predict that positively tilted facets and GBs ( $\vec{E} \cdot \vec{n} < 0$ ) are more stable than negative tilted ones ( $\vec{E} \cdot \vec{n} > 0$ ). Thus, one would expect to see some grain boundaries along a bamboo type structure to be more “grooved” than others [9]. Cathode voiding and anode hillocking are common in drift velocity experiments, in agreement with our case B model. It therefore appears that at least qualitatively, the two variants of the IG void simulation presented here have some experimental support.

More interesting, and somewhat surprising, is the commonality of topologies for a transgranular edge void obtained with our non-mass-conserving (A) model and Schimschak and Krug's [3, 4] mass-conserving model. The mass conservation in [3, 4] is due to the periodicity in the boundary conditions, for boundaries about 2 line thicknesses away from the void center. In our model, the non-mass-conserving boundary conditions  $K_s = 0$ , are imposed at a 3 times larger distance. The similarity of behavior with respect to the overhang may be due to the fact that the overhang is created by local diffusivity field effects, being less affected by distant boundary conditions.

## 4 Conclusion

In conclusion, we model the surface evolution of a bamboo-type surface subjected to surface diffusion and electromigration, under two types of boundary conditions: mass-conserving and non-mass-conserving. Surprisingly, our non-mass-conserving model for a transgranular edge void yields similar evolution topologies to those of existing mass-conserving models, indicating that local diffusivity effects are weakly dependent on boundary conditions imposed at distances greater than a few time line thickness. If this conclusion is correct, the evolution of an intergranular edge void (two-grain domain) under mass-conserving and non-mass-conserving conditions may be well matched with corresponding experimental observations, explaining cathode voiding and anode hillocking in mass-conserving experiments, and surface thinning in non mass-conserving ones.

**Acknowledgement:** We wish to thank Dr. Igor Ravve for his help with the simulations.

## References

- [1] W.W. Mullins, J.Appl. Phys. 28 (1957) 333.
- [2] see e.g. B. Sun and Z. Suo, Acta Mater. 45 (1997) 4953.
- [3] M. Schimschak and J. Krug, Phys. Rev. Lett. 78 (1997) 278.
- [4] M. Schimschak and J. Krug, J. Appl. Phys. 87 (2000) 695.
- [5] M. R. Gungor and D. Maroudas, J. Appl. Phys. 85 (1999) 2233.

- [6] E. E. Oren and T. O. Ogurtani, MRS Symp. Proc. 695 (2002) 209.
- [7] A. Averbuch, M. Israeli, M. Nathan and I. Ravve, J. Comp. Phys. 188 (2003) 640.
- [8] R. A. Augur, R. A. Wolters, W. Schmidt, A. G. Dirks and S. Kordic, J. Appl. Phys. 79 (1996) 3003.
- [9] L. Arnaud, T. Berger and G. Reibold, J. Appl. Phys. 93 (2003) 192.

## FIGURE CAPTIONS

Figure 1: (a) single grain domain with triangular edge voids, and (b) two grain domain with positively tilted grain boundary. The electric field is positive from left to right in both domains.

Figure 2: Surface evolution of transgranular voids: (a) strong electric field ( $\alpha = 50$ ), non-mass-conserving case; (b) moderate electric field ( $\alpha = 20$ ), mass-conserving case.

Figure 3: Surface evolution in two grain domain with tilted grain boundary (IG void) under surface diffusion only (zero electric field); (a) non-mass-conserving case; (b) mass-conserving case.

Figure 4: Surface evolution in two grain domain with positively tilted grain boundary under surface diffusion and weak electric field ( $\alpha = 10$ ); (a) non-mass-conserving case; (b) mass-conserving case.

Figure 5: Surface evolution in two grain domain with negatively tilted grain boundary under surface diffusion and weak electric field ( $\alpha = 10$ ); (a) non-mass-conserving case; (b) mass-conserving case.

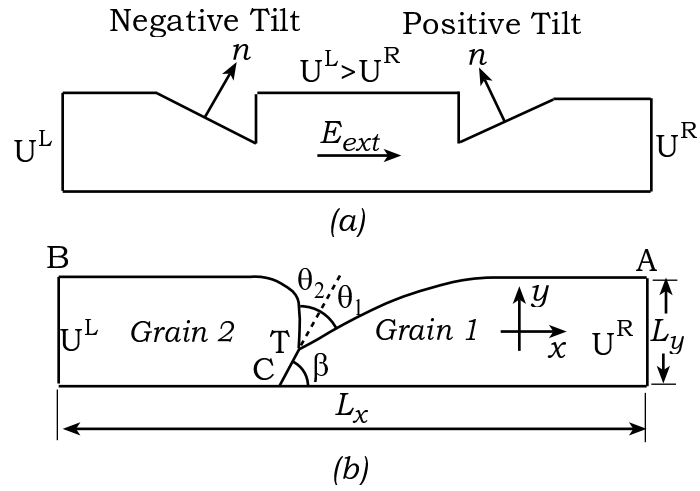


Figure 1:

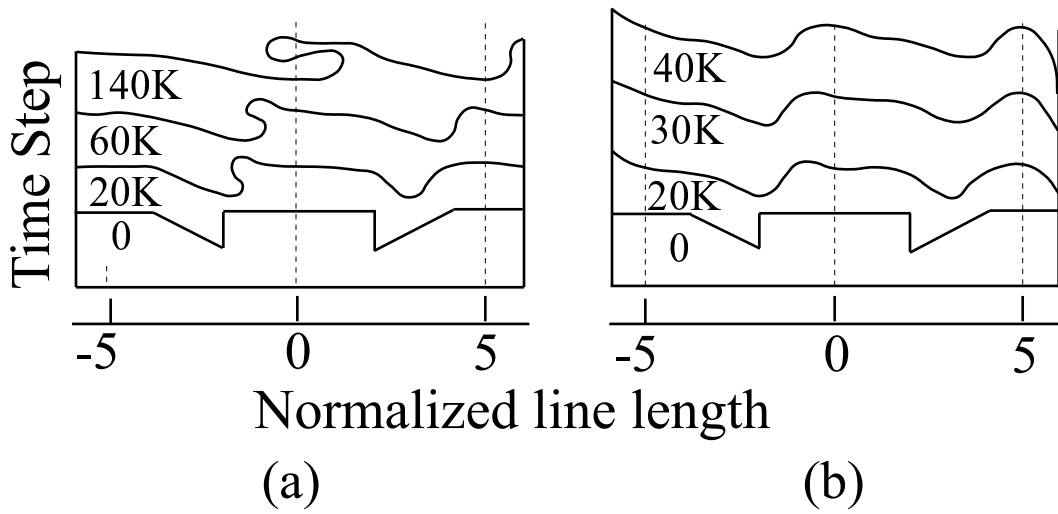


Figure 2:

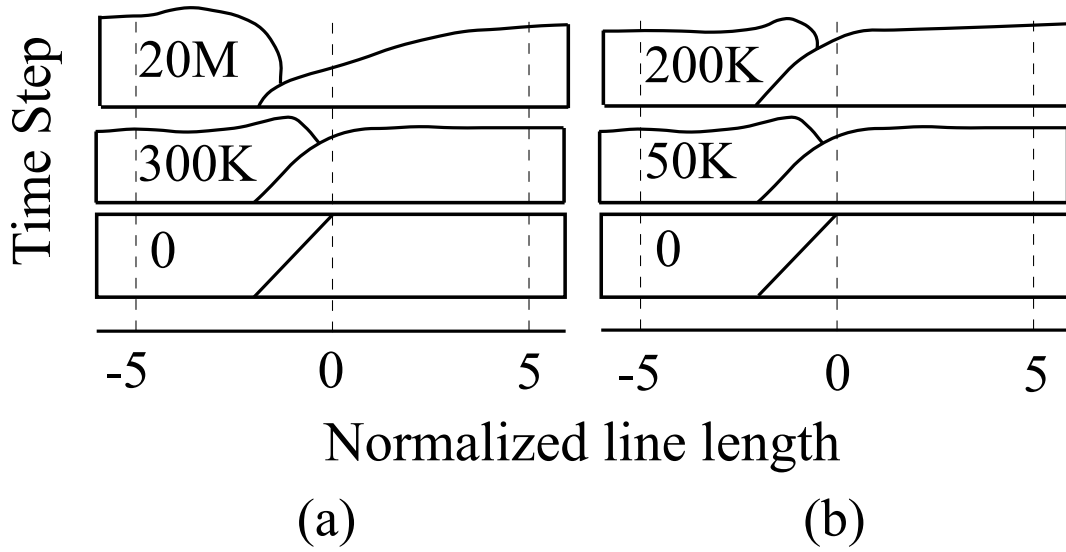


Figure 3:

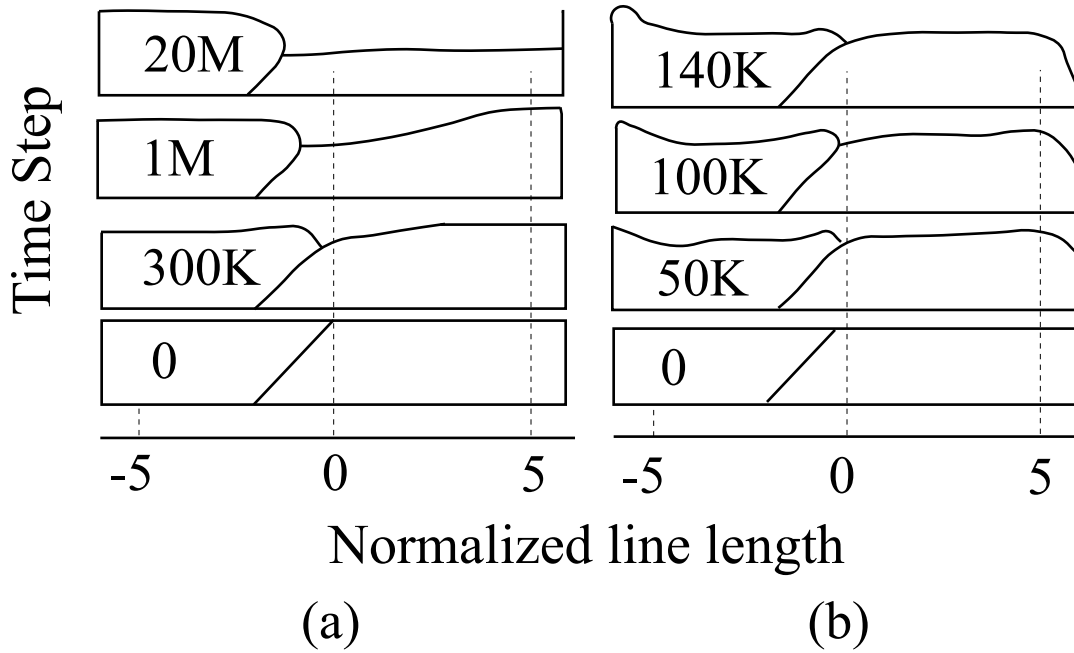


Figure 4:

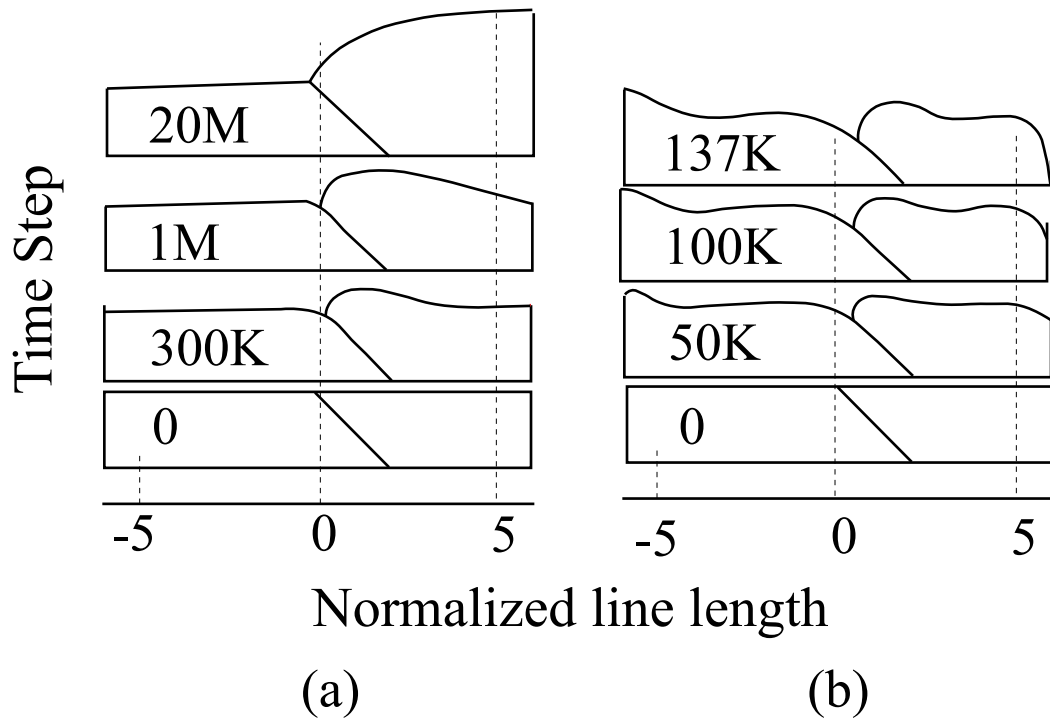


Figure 5: